CONTROL OF SOLIDIFICATION STRUCTURE IN VAR AND ESR PROCESSED ALLOY 718 INGOTS

K. O. Yu* and J. A. Domingue**

* PCC Airfoils, Inc., Beachwood, Ohio.
**Special Metals Corporation, New Hartford, New York.

ABSTRACT

Solidification in VAR and ESR processed Alloy 718 ingots was reviewed. Effects of melting phenomena and heat transfer condition on ingot structures were described. Moreover, formation mechanisms and prevention strategies for three major types of defect, i.e., sonic defect, freckles, and white spots were treated in detail. Finally, recent process developments, e.g., hot-topping of VIM electrodes, digital drip short control for VAR, and automatic melting rate control for both VAR and ESR were discussed.

1.0 INTRODUCTION

In the discussion of solidification phenomena of Alloy 718, caution must be observed to first distinguish among the diverse compositional grades collectively designated "718", along with corresponding diverse applications. Differences are substantial from non-turbine to structural casting (low gas content), to wrought rotating disk (high niobium) versions of the alloy. Much of the review which follows arises from the authors' experiences with 508mm (20-inch) diameter consumable melted ingots processed to billet stock for fabricating aerospace turbine disks.

In North America, the double vacuum melt process of vacuum induction melting (VIM), followed by vacuum arc remelting (VAR) for wrought components, is the sole qualified method of manufacture for rotating parts. By far the larger volume of rotor quality Alloy 718 goes into disks, and its usage thereof exceeds that of any other aerospace superalloy. In recent years, there evolved strong economic motivation to enhance engine performance and efficiency by extending stress and temperature capabilities of disks. To this effort, various alternatives for the secondary melt process are under investigation. For example, electroslag refining (ESR)[1] and electron beam cold hearth refining (EBCHR)[1] show promise for improving fatigue properties by reducing inclusion size and frequency. Homogeneity and structure improvements related to strength and ductility are available from vacuum arc double electrode remelting (VADER)[2,3] and from atomization for powder metallurgy (PM). Developmental activities reach back to the primary melt process and even to raw materials processing

Superalloy 718—Metallurgy and Applications
Edited by E.A. Loria
The Minerals, Metals & Materials Society, 1989

for the purpose of stabilizing secondary melting with consistent electrodes.

The major result of these investigations, to date, is the qualification of a VIM, ESR, and VAR triple melt process now in production for selected high pressure turbine (HPT) disks. The intermediate ESR step not only provides a product with smaller and fewer nonmetallic inclusions, but also provides sound, consistent electrodes for better controlled VAR melting and solidification. Much of the added processing expense of triple melt is reclaimable as improved yield in the form of reduction of melt related defects in billet.

The typical 508mm diameter ingot requirement for wrought aerospace Alloy 718 presents formidable problems for three major types of defect, i.e., sonic defect, freckles, and white spots. This paper reviews solidification in both VAR and ESR processed Alloy 718 ingots. The effects of critical process parameters on ingot structures are described. Moreover, formation mechanisms and prevention strategies for freckles and white spots are treated in detail. Finally, recent process developments, e.g., hot-topping of VIM electrodes, digital drip short control for VAR, and automatic melting rate control for both VAR and ESR are discussed.

2.0 PHYSICAL METALLURGY

The composition of Alloy 718 is given in Table I, including precipitation strengthener (Al, Ti, Nb) levels and other special requirements for rotating part quality. The solidification range is generally from 1204 to 1343°C (2200 to 2450°F) with some variation with compositional grade, especially in the solidus.

TABLE I. COMPOSITION OF ALLOY 718
(WEIGHT PERCENT) FOR ROTATING PARTS

Cr	Fe	Nb+Ta	Mo	Ti	Al	C	B	Ni
18.1	17.5	5.35	3	0.95	0.5	0.30	0.003 max	Balance

Chromium and molybdenum are added for the usual superalloy corrosion resistance and solid solution strengthening, respectively, while niobium serves the added function of stabilizing the carbide phase to the MC type. Although it is austenitic, Alloy 718 differs from gamma prime strengthened superalloys, in that, under a wide range of solidification condition, a metastable hexagonal Laves, $Fe_2(Nb,Ti)$, phase occurs. Evidence of Laves has been found even in atomized powder.[4] This is not the typical superalloy eutectic gamma prime, which is merely a shift away from equilibrium composition within a stable phase field, and which is redistributed by homogenization practice. Laves is a distinct phase which, after solid state solutioning, does not reprecipitate in any form with any aging treatment. What is important about Laves is that its formation is a concentrating mechanism for slow diffusing niobium. This makes the alloy unresponsive to homogenization treatment within a reasonable time. Niobium, once concentrated during solidification, reappears after solutioning and aging as regions of excess nickel rich phases, and all commercial Alloy 718 has some

measurable banding. The equilibrium precipitation phase, orthorhombic delta $Ni_3(Nb, Ti)$ forms by aging in the (871 to 982°C (1600 to 1800°F) range. Delta is acicular in morphology on aging and deleterious to properties. The preferred precipitates are Ni_3X-type body centered tetragonal gamma double prime (major) and face entered cubic gamma prime (minor). These develop at temperatures below the delta formation region, are not thermodynamically stable phases, solution above 1010°C (1850°F) and revert to delta on aging at 871 to 982°C. Relative to solidification study, the situation is simplified in that it is the distribution of niobium itself, and not the various phases which niobium appears in, which is the true measure of homogeneity. The complicating factor is that etchants are sensitive to phase differences more than to elemental concentration differences.

3.0 MELTING PHENOMENA

The heat generated in the VAR process results from the electric arc between the bottom surface of the electrode and the ingot top surface. A vacuum arc is an electrical discharge which depends on vaporization and ionization of electrode material for sustenance in an ambient atmosphere, wherein, the mean-free path of an ion or an electron in the residual gas is much greater than the dimensions of the discharge.[5] The arc behavior and electrode melting rate of VAR are strongly influenced by the type and pressure of the gas that is present in the furnace chamber. Zanner[6] et. al., showed that when the CO gas was presented in the chamber (1.33 to 133 Pa), ingot melting rate could be reduced by as much as 25% and arc configuration could be changed from one producing uniform heat distribution on the electrode surface (diffuse arc for a low gas pressure) to one with a concentrated heat distribution (constrained arc for a high gas pressure). Moreover, in order to sustain this effect, the CO pressure must increase with increasing current density. For industrial size VAR, the pressure during melting is about 0.133 to 1.33 Pa (10^{-3} to 10^{-2} torr).

In ESR, the electrode is remelted by passing a current through it into a molten slag which is resistively heated and which, in turn, melts the electrode. The electrode melting rate depends strongly on the slag composition as well as on the amount of slag being remelted. The commonly used slag composition for Alloy 718 is 70/15/15 (CaF_2-CaO-Al_2O_3).[7]

Yu and Flanders[8] found that both the melting rate and specific energy consumption during the steady-state operation of both VAR and ESR are linear functions of power input. The melting rate always increases with power input level. Specific energy consumption, however, exhibits a more complicated relation with power input. It is generally true that specific energy consumption decreases with an increase of power input for VAR. In the case of ESR, however, the specific energy consumption can either decrease or increase with an increase of power input, depending on the alloy system being melted. For Alloy 718, the specific energy consumption of ESR increases with the power input, whereas, it decreases in VAR. Furthermore, this difference in specific energy consumption has

a significant influence on freckle formation tendency.

4.0 INGOT STRUCTURE

The VAR and ESR ingot structure depends to a large extent on the thermal history of the ingot. Yu and Flanders[8] reported that the significant difference in heat transfer characteristics between the two processes resulted in considerable differences in the ingot pool profile and grain growth pattern (Figure 1) which then had direct impact on macrosegregation formation tendency and forgeability.

Yu also showed that based on the measured dendrite arm spacing (DAS) data and on the known relationship between DAS and local solidification time, an approximate picture of mushy zone shape and the general trend of the change of mushy zone shape with melting rate can be obtained (Table II). In general, V-shaped pool profiles with nonuniformly distributed mushy zones are found in ESR ingots, whereas, shorter and relatively uniformly distributed mushy zones associated with U-shaped pool profiles are found in VAR ingots. Moreover, VAR data in Table II also shows that high power input and melting rate resulted in small DAS; i.e., fast cooling rate and short local solidification time, but deep mushy zone depth. This statement is also true for ESR processed ingots[9].

Because the effect of the slag skin, a smooth surface is usually obtained for ESR ingot. During VAR melting, condensed metal vapor and splattering droplets form a crown (or collar) (Figure 2) on the top edge of the ingot. With the increase of ingot height during melting, a shelf is formed at the surface periphery of the ingot. Hence, the resulting ingot surfaces are usually not smooth and are composed of several layers. The presence of top collar and surface shelf during VAR melting not only has a detrimental effect on ingot hot workability, but also results in a possibility to form white-spots.

5.0 Types of Defects

5.1 Microsegregation

Microsegregation is the most common indigenous defect and is, in fact, natural to the dendritic solidification mode. With increasing local solidification time, primary dendrite "spines" and secondary dendrite "arms" grow larger, as does the interdendritic space which contains the lower melting precipitate-primary phase eutectic, a material enriched in niobium. Depending on the rate of solidification, microsegregation may or may not be actually observable macroscopically. This may confuse the inexperienced observer with true macrosegregation, which is a physical displacement of solute in the mushy zone. More explicit names for microsegregation in wrought structures are "remnant dendritic pattern" and "residual dendritism".

It is not feasible to inspect routinely for segregation in wrought products at cast ingot stage. Therefore, no statistical capability analysis is known to have been done and no standards are in effect for as-cast dendrite arm spacing. At billet macro inspection stage, no attempt is made to quantify the extent of remnant dendrite pattern. Rather,

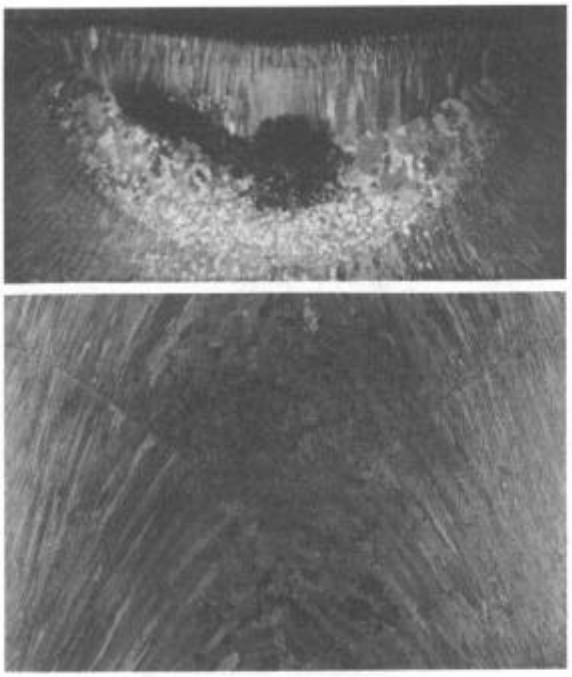

(a)

(b)

Figure 1. Ingot pool profiles and grain growth patterns of (a) VAR and (b) ESR[8].

TABLE II. Estimated mushy zone shapes of ESR & VAR processed ingots.[8]

Ingot Type		VAR	VAR	ESR
Power Input Kw		125	200	240
Melting Rate Kg/Hr.		180	322	273
Ingot Diameter mm		508	508	432
Dendrite Arm Spacing μm	C	131	114	113
	E	101	104	74
Mushy Zone Thickness* mm	C	123	146	167 (152)**
	E	57	115	48 (40)**
Mushy Zone Shape		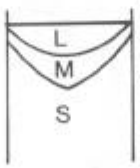	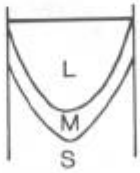	

photographic references are used to enforce a rule of thumb that any pattern "marbled" enough to be possibly mistaken for, or not fully distinguishable from, macrosegregation is rejected. Figure (3) shows residual dendritism in billet, from a 508mm diameter VAR ingot which passed inspection. The structure is typical of ingot top regions. The more rapid solidification in stool-affected region usually gives a residual dendritism in billet which is invisible to the unaided eye.

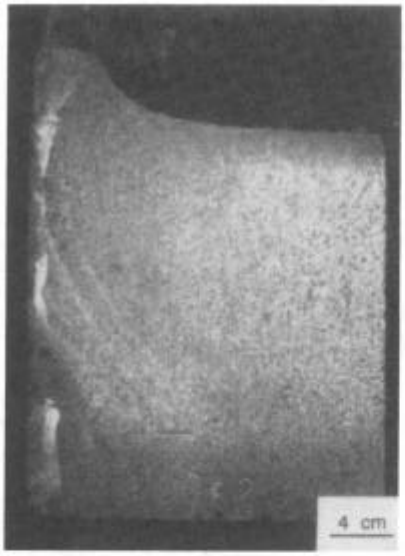

Figure 2. Crown and Shelf of A VAR ingot.

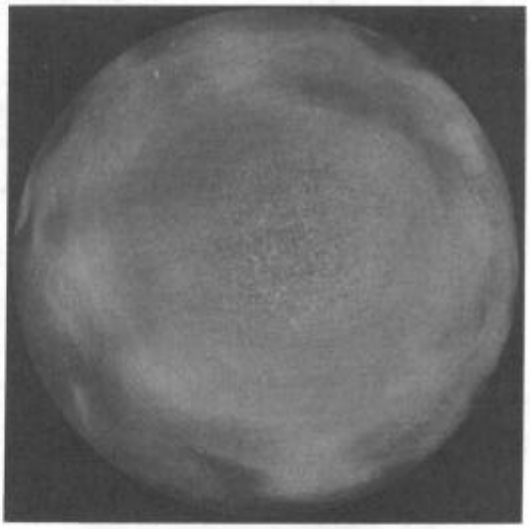

Figure 3. Residual dendritism in VAR billet.

5.2 Macrosegregation

The primary purpose of VAR and ESR processing is to improve ingot compositional and structural homogeneity as well as forgeability by adjusting ingot structure. From this point of view, the control of macrosegregation is the most important quality factor of VAR and ESR ingots. Three types of macrosegregation have been observed in billets that converted from VAR and ESR processed ingots: tree rings, freckles, and white spots.

5.2.1 Tree Rings

Tree rings are concentric rings in the transverse macrostructure. The differential etching is associated with a minor gradient in chemical composition or fluctuations in dendrite orientation. No observed detrimental effect on material mechanical properties due to the presence of tree rings has been reported. Hence, they were not included in the following discussion.

5.2.2 Freckles

Freckle is the most common type of positive macrosegregation to which VAR and ESR ingots are prone. Flemings and coworkers[10-12] showed that freckles are resulted from flow of solute-rich interdendritic liquid in the mushy zone during solidification. Movement of this interdendritic liquid occurs as a result of solidification contraction, of gravity acting on a fluid of variable density, and of electromagnetic forces.

For Alloy 718, Domingue et. al.,[13-15] showed that freckles (Figure 4) are dark-etching spots that appear in the center to mid-radius of forged billets. These spots are rich

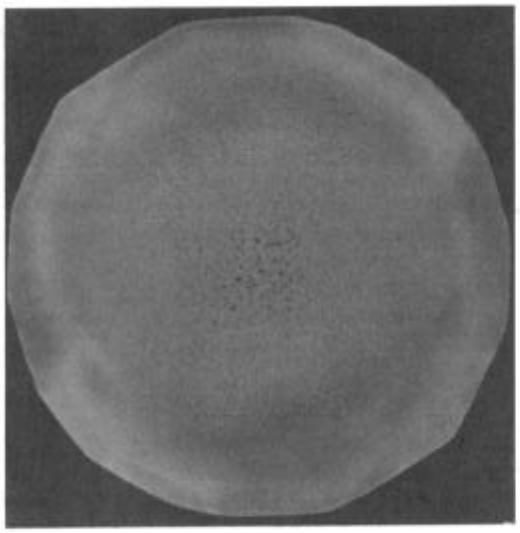

Figure 4. Freckles in ESR-processed billet

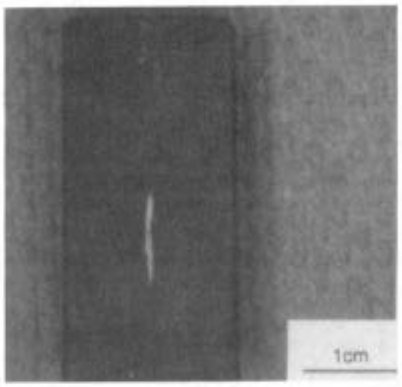

Figure 5. White spot in VAR-processed billet.

in niobium and contain excessive amounts of a Laves phase. The sizes of freckles are much larger than the dendrite arms of as-cast ingots. The size factor, combined with the negligible solid state diffusion rate of niobium, makes freckles virtually unmovable by any amount of thermomechanical processing. The effect of freckles on properties is to reduce yield strength and ductility.[16] Ingot processed at a relatively high melting rate are more often affected, and as ingot diameter increases, the phenomenon is more likely to occur.

Yu and Flanders[8] demonstrated that the V-shaped pool profile with a prolonged mushy zone can enhance the intensity of interdendritic fluid flow in an ESR ingot. On the other hand, the U-shaped pool profile with a shorter and more uniformly distributed mushy zone in VAR ingots indicates that the formation of freckles will require higher melting rates in VAR than in ESR. Moreover, Yu[9] indicated that the differences of local solidification time and dendrite arm spacing between the center of the ingot and surface are decreased with an increase of melting rate in VAR, whereas, they are increased in ESR. Thus, with an increase of power input level, the increase of the probability for freckle formation in ESR is much higher than in VAR. As discussed in Section 3.0, specific energy consumption of ESR-processed Alloy 718 increases with power input, whereas, it decreases with power input in VAR. Thus, with an increase of power input, the corresponding increase of heat input into the molten pool in ESR is much higher than in VAR, which increases the probability of freckle formation. This correlation is substantiated by the fact that the typical production size of VAR processed Alloy 718 ingots is 508mm (20 in) diameter, while 432mm (17 in.) diameter ingots ESR processed at comparable melt rates will have freckles unless an adequate solidification control strategy is employed.

5.2.3 White Spots

White spots (Figure 5) are randomly distributed, discrete nonetching shiny areas, which are lean of niobium.[14] White spots encapsulated by oxide and/or nitride envelope are called "dirty" white spots, whereas, those with clean interfaces with the matrix are referred to as "clean" white spots.[1] Surface white spots have adverse effect on component mechanical properties, and dirty white spots at any location reduce the low cycle fatigue life. Ingots processed at a relatively low melting rate are more often affected, and, in general, the problem is localized in the portion of the ingot product influenced by hot-topping. VAR processed ingots are more prone to this phenomenon than ESR ingots.

The reason for the formation of white spots is exogenous material falling into the pool and remaining unmelted. Major sources of these exogenous fragments are crown and shelf on the top edge of VAR ingots and dendrites from VIM electrodes.[15,17,18]

During VAR melting, pieces of crown and shelf may be undercut by the arc due to arc instability and fall into the molten pool. The chemical composition of the shelf is usually lean in niobium and rich in oxides and nitrides. Figure 6 shows a transverse billet section with a nonetching shiny ring of shelf at its lateral surface. The chemistry of this shelf is lean in Nb and Ti and similar to that of the white spot.

In VIM electrode casting, solidification shrinkage occurs in the central part of the electrode causing a pipe and porous region to form along the center line. During the remelting, some of the porous material may be dislodged and fall into the molten pool. According to solidification theory, dendrites in these porous regions are lean in niobium and have a higher melting point than the interdendritic material. Hence, this is the last material to be melted.

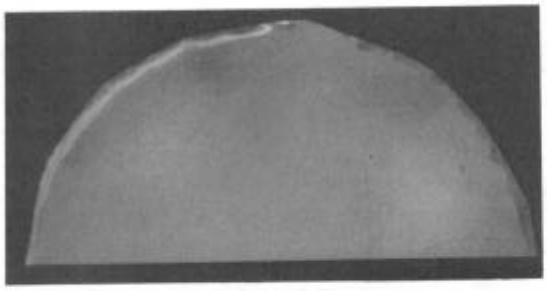

Figure 6. Shelf in VAR billet.

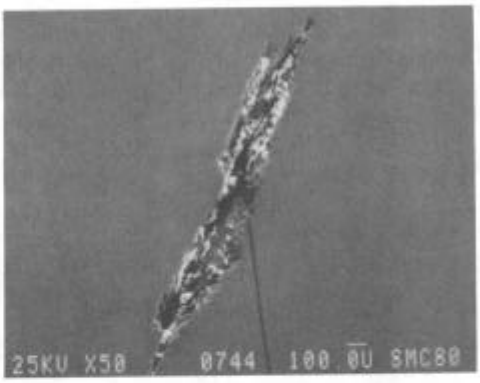

Figure 7. Sonic defect in billet.

5.3 Sonic Defect

Most ultrasonic indications (Figure 7) in wrought Alloy 718 upon examination are found to be minute cracks associated with

magnesium and aluminum oxides and titanium nitrides. These are the stable impurities emerging from the VIM environment and preserved through secondary melting. Indications can be from voids containing no inclusions, but this is rare, and implicates conversion practice. Aerospace ultrasonic rejection standards range from 2 to 0.8mm (5/64 to 2/64 inch) cavity, as the stress applied to the component increases.

During VAR and ESR, nonmetallic particles can be entrapped by the rising solidification front. In VAR, inclusion removal is by transport and adhesion of nonmetallics to the ingot-mold wall interfacial region. Removal is favored by increasing pool depth, decreasing advance of solidification front, and minimum pool turbulence. The mechanism of inclusion removal in ESR is by dissolution into the slag cover. It is generally agreed that ESR has a superior cleanliness compared to VAR.[1]

Another mechanism for sonic defect formation is provided by white spots. In fact, nonmetallic inclusions causing ultrasonic indications in VAR billet are typically associated with "dirty" white spots. Because of the slag action and the absence of crown/shelf associated white spots, the frequency of ultrasonic indications in ESR billet is less than for VAR billets.

6.0 PROCESS CONTROL

6.1 Primary Melting

Control of solidification of wrought Alloy 718 begins with the manufacture of the consumable electrode. The simple strategy in effect is that maximum soundness and consistency of electrodes allows maximum "fine tuning" of consumable melting parameters. Reproducibility from electrode to electrode aids in determining optimum consumable melting set points with a minimum of replication. Minimizing the nonmetallic content of the electrode minimizes the potential for billet ultrasonic indications. Marked evidence for this strategy is the reduction in sonic defects and inclusion initiated fatigue failures in VIM-ESR-VAR as compared to VIM-VAR Alloy 718.

Aspects of VIM under development are: 1) SPC (Statistical Process Control) of VIM parameters; 2) Teeming practice, including filters; 3) Mold preparation, including hot tops.

The advantages and disadvantages of porous ceramic filters in the VIM tundish have been reported,[19-22], and the practice is used in the production of superalloy "remelt sticks" for investment casting. The reported level of cleanliness of filtered VIM casting material, as measured by the EB button test, is comparable to that of VIM + VAR in wrought alloys. It has yet to be determined what the long-range advantage would be in going into VAR with an electrode of this low inclusion content, and how this advantage weighs against the added process control required for successful filtering of the larger VIM heats generally poured for wrought alloys.

Both primary and secondary pipes are normally seen in VIM electrodes. The primary pipe cavity can extend several ingot diameters from the top of the ingot and be up to 1/2 the

diameter of the ingot in cross-sectional area. These pipes have adverse effects on ingot structure for two reasons. First, during remelting, unsound electrodes increase the arc instability (VAR). Second, the probability of porous materials falling into the molten metal pool (VAR and ESR), which increases the probability for the formation of white spots.

Several methods are used to reduce the size of the electrode shrinkage pipes. Secondary pour or back fill with the last liquid from the crucible (which is commonly used for the hot-topping of small size "remelt sticks") runs the risk of implanting contaminants into electrode regions which are virtually uninspectable in production. Pouring the metal with low superheat and at slower rates are extremely difficult to achieve because the tundish is not separately heated and very low pour rates are not economically feasible. Hot-topped molds show more promise. Geometric constraints within the vacuum pour-chamber may, in some cases, require mold inserts which reduce electrode weight. Exothermic hot-top materials are generally avoided.

There is a movement in the industry to bring VAR and ESR under statistical process control with digital computer monitoring and disk storage of melt variables.[23] This trend in development is strongly motivated by the need to resolve the complexity of sonic defect and white spot formation. Hot-topping of VIM electrode can reduce the size of shrinkage pipe and, hence, provide a structurally consistent electrode for both VAR and ESR. This will accelerate the development of statistical control of the VAR and ESR melt, and lead to a reduction in white spot and sonic defect frequency.

6.2 Prevention of Freckles

When freckles are found in Alloy 718 disk materials, the first reaction of the process engineer is to decrease the melt rate. Yu et. al.,[15] indicated that, although a high melting rate results in a high cooling rate and short local solidification time, the associated long mushy zone and strong interdendritic fluid flow often cause the formation of freckles. On the other hand, a low melting rate favors a short mushy zone and weak interdendritic fluid flow; however, the resultant low cooling rate and long local solidification time cause coarse dendritic structure (exaggerated micro-segregation, which cannot completely break down under open die forging) and poor ingot surface. A better way to control the formation of freckles is by improving the ingot heat extraction rate. As the heat extraction rate is increased, the ingot cooling rate is increased and the local solidification time is decreased. This results in ingots possessing a shorter mushy zone, less intensive interdendritic fluid flow, and lower freckle formation tendency.

The above mentioned theory can be further explained by the following equation[8]:

$$\dot{\xi} = (T_L - T_S)\ V/L_M \qquad (1)$$

where, $\dot{\varepsilon}$ is the cooling rate at the center of the ingot; T_L and T_S are liquidus and solidus temperatures, respectively; V is ingot casting speed (which is related to electrode melting rate); and L_M is the length of the mushy zone at the center of the ingot. Equation (1) indicates that cooling rate $\dot{\varepsilon}$ decreases with a decrease of V/L_M ratio. In general, when melt rate and, hence, casting speed V is decreased to a lower level, the mushy zone thickness L_M decreases. However, the heat transfer condition in current industrial VAR and ESR operation is that L_M does not proportionately decrease with V (i.e., V/L_M ratio decreases instead of remains constant), which results in an ingot cooling rate that decreases with a decrease of melt rate. The consequence of this strategy is that a lower melt rate results in a smaller mushy zone size but not necessarily a lower freckle formation tendency. Conversely, if a strategy of increasing ingot heat transfer rate instead of reducing melt rate is employed, a smaller mushy zone size as well as shorter local solidification time (i.e. higher cooling rate) results. This strategy decreases the freckle formation tendency.

6.3 Prevention of White Spots

The formation of white spots should be minimized by decreasing the frequency at which exogenous material falls into the pool and by increasing the probability of remelting before entering the mushy zone.[15]

The availability of porous material to fall into the molten pool can be effectively diminished by reducing the extent of the primary shrinkage cavity (pipe) in the electrode. Moreover, a solid electrode has transverse surface characteristics favorable to arc stability which, in theory, reduces the probability of the shelf being undercut and falling into the pool. Hot-topping VIM electrodes and forged ESR ingots in the triple melt may fulfill these requirements.

Power input at the main burn-off region should be maintained at a relatively high level to maintain a deep and superheated molten pool in which the exogenous materials have more chance to dissolve. In order to achieve this goal, however, care must be taken to assure that the high level power input melting is always accompanied by an improved heat transfer rate to avoid the formation of freckles. This theory is also explained by equation (1). When melting rate and, hence, casting speed V is raised to a higher level, both the liquid metal pool depth and the mushy zone thickness L_M also increase. If the heat transfer condition is such that L_M increases proportionately with V, (i.e., V/L_M ratio keeps constant), the average cooling rate is a constant regardless of the values of casting speed. In this case, although a deep liquid metal pool favors the remelting of those exogenous materials, and thus eliminates them as sources of white spots, the longer L_M represents a larger mushy zone, stronger interdendritic fluid flow, and higher tendency for freckle formation. However, if an improved heat transfer condition can be maintained simultaneously with the increase of power input, a shorter mushy zone depth L_M, higher V/L_M ratio, and higher cooling rate is be obtained. In this way, the tendency

for the formation of white spots is decreased, but not at the expense of higher freckle formation tendency.

During VAR operating, the arc gap should be controlled as tightly as possible to reduce the amount of condensed metal vapor and splattering droplets that deposit on the crucible wall to form shelf. Consequently, a thinner shelf, which takes less time to melt after it falls into the molten pool, results.

6.4 Control of Crucible Heat Transfer Rate

As stated in Sections 6.2 and 6.3, improving ingot heat transfer condition is a vital necessity for the control of freckles and white spots. In order to better control the ingot structure, a detailed description of the heat transfer characteristics of the copper crucible during ingot solidification of the two processes must be examined.

The flow of heat through ESR and VAR crucibles is a complex process and depends on several factors; e.g., slag skin thickness (ESR), helium pressure (VAR), shrinkage gap width, cooling water flow rate, and crucible surface condition (Figure 8). Yu[24] theoretically analyzed the fundamental heat transfer mechanisms in the VAR and ESR crucibles and quantitatively estimated what possible gains could be obtained from changes in those factors.

Yu's results demonstrated that, in most regions of the ingot lateral surface, the VAR process has a higher heat transfer coefficient than that of ESR, except at the location very near the top of the ingot (Figure 9). The heat transfer coefficient of VAR can be improved by increasing the helium pressure in the shrinkage gap between the ingot surface and the crucible wall. Higher power input results in better contact between the top crown and crucible wall, forming a seal to prevent the leakage of helium gas. This results in a higher helium pressure. Higher helium flow rate also yields higher helium pressure. For ESR, the most important factor controlling the heat transfer coefficient is the slag skin thickness. The heat transfer coefficient decreases with an increase of slag skin thickness. Since the thickness of slag skin increases with a decrease of melting rate, it is difficult to be independently controlled like the helium pressure in the VAR operation. Therefore, the control in ingot cooling rate is more difficult in ESR than in VAR.

This theoretical analysis was confirmed by the experimental data of Hosamani et. al,[25] who investigated the effect of helium gas pressure on the cooling rate and structure of 6-inch diameter VAR processed Alloy 718 ingots. Their results showed that 17% more heat could be extracted by the cooling water, and about 36% decrease in molten metal pool depth was obtained with 60mm helium gas between the ingot and crucible. Moreover, it was found that dendrite arm spacing of ingots with helium gas cooling was significantly finer than that of ingots without helium gas cooling.

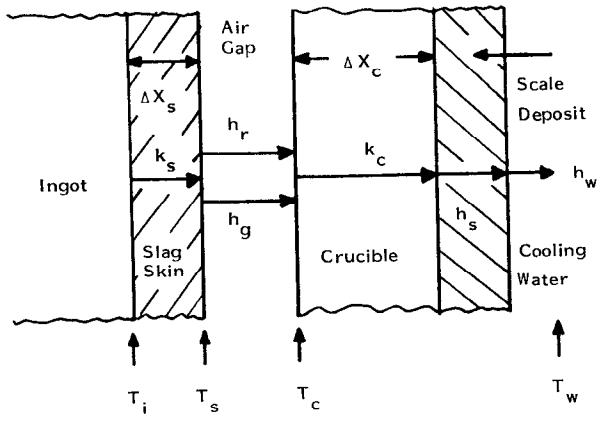

E S R

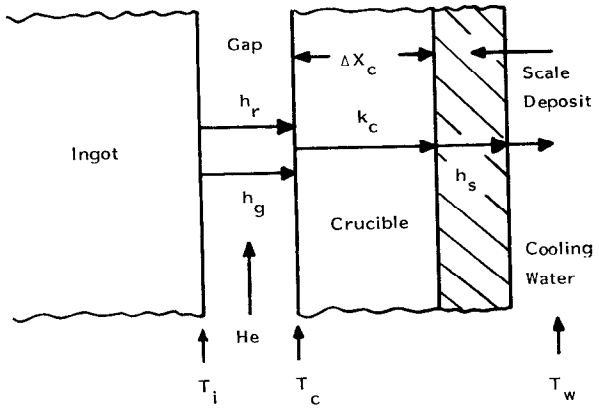

V A R

Figure 8. Schematics of the heat transfer resistance from ESR & VAR ingot surfaces to the crucible cooling water.[24]

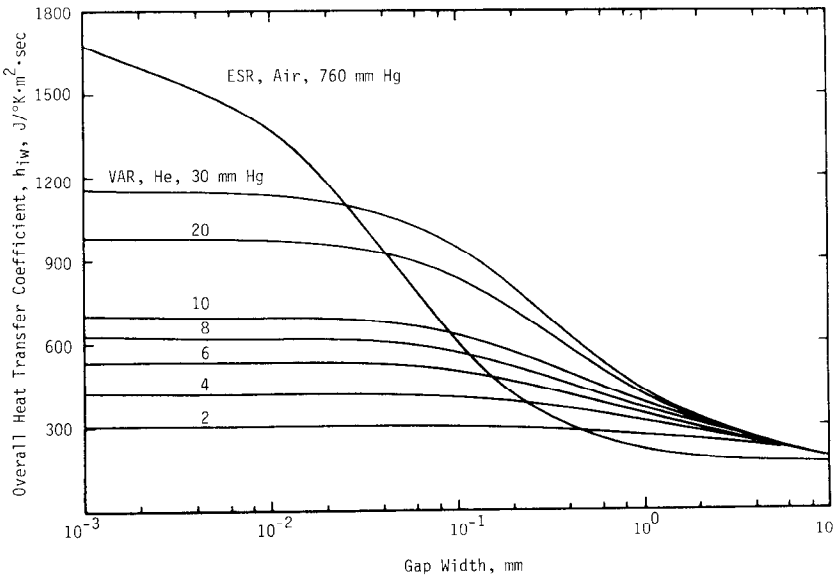

Figure 9. The Effect of Gap Width on Heat Transfer Coefficient for ESR & VAR at Various Gas Pressures

6.5 Arc Gap Control For VAR

In VAR, the arc gap has a significant effect on heat transfer condition and resulting ingot structure. Increasing arc gap increases radiational heat loss from the arcing surfaces, and additional energy loss from increased tendency for arcing to mold wall. Thicker shelf and higher frequency of other defects associated with shallower pool result. However, some minimum arc gap must be maintained for negligible probability of solid electrode touching pool, which is an equally catastrophic diversion of the energy input. Any non-symmetric distribution (constriction) of the arc results in non-concentric pool profile. Concentration of the arc to the center promotes shelf,and concentration of the arc to the circumference promotes arcing to wall and crown-shelf instability.

Control of the arc gap must be more precise and responsive than that achieved merely by setting the electrode drive speed based on electrode to ingot cross section ratio (fill ratio) and based on a preset reference voltage. During VAR remelting, the droplets do not simply fall into the pool, but stretch down and short out the arc current for times in the micro- to millisecond range. The frequency of drip shorts and of hash (positive voltage spikes associated with drop shorts) is inversely proportional to arc gap. Thus drip short measurement forms the basis for precision arc gap control. Drip shorts and related arc phenomena have been characterized and reported extensively by Zanner and associates.[26,27] When billet or parts are rejected for melt related defects, arc gap variation is highly suspect.

Melt conditions giving use to or resulting from constrained arcs have an effect in addition to disturbing pool symmetry. The relationship between the arc gap and the measured drip short count is perturbed whenever the droplets are not forming and falling randomly across the entire electrode cross section. This sends erroneous signals to the electrode drive mechanism. Especially serious is non-planar electrode surface, from which droplets coalesce and descend from the lowest point or points. Non-uniform cross section, as with variable electrode shrinkage cavity, is also a problem. Even under ideal measurement conditions, the tolerable limits of duration and frequency of departing from optimum arc gaps are not fully understood.

6.7 Control of Melting Rate

An average melt rate can be calculated from the weight of an electrode and the time it takes to melt, with corrections for end effects. Time trends in the average melt rate provide a useful check against drift and shift in the measurement of melt control parameters. A quasi-instantaneous melt rate can be obtained by suspending the electrode from a load cell. Feedback and response systems for closed loop melt rate control have been developed by Alloy 718 producers and are commercially available from VAR furnace manufacturers. Although some lag always exits in the response of a closed loop melt rate control,. a melt rate monitoring load cell is advantageous for early detection of excessive variance in melt parameters, by

acting as a check on the other instrumentation or by suggesting change in some unmeasured characteristic. Measurement of weight is proportionately more reliable than, for example, measurement of current.

In ESR, with the long static mold configuration, it is difficult to continuously monitor the depth of slag cover. This makes closed loop melt rate control virtually imperative for reasonable solidification control of Alloy 718. Furthermore, power input changes are required whenever any fluctuation in the cooling water flow momentarily raises or lowers the temperature of the slag. The same time response problem experienced in VAR exists for ESR. However, some lag is tolerable, because thermal lag in warming and cooling of the slag mass hinders abrupt changes in melt rate. There is more variance in the melt rate data in ESR than in VAR as evidenced quite clearly by the wider noise band in the charted melting rate trace. One possible contribution to this noise is the buoyancy force of the slag, which for 356mm (14 inch) and 432mm (17 inch) diameter electrodes is 0.68Kg (1.5 pounds) and 1Kg (2.3 pounds) respectively per 2.54mm (0.1 inch) change in immersion depth. This is in the same order of magnitude as the limit of detectibility of a 4546 Kg (10,000 pound) capacity load cell, which is about 0.45 Kg (1 pound).

The electrode is positioned to ideally just barely make contact with the top of the slag, with a meniscus seal between slag and solid electrode formed by surface tension. With the electrode in this position, measurable noise is documented on the voltage chart trace due to the partial electrical contact. This forms the basis for a programmable voltage "swing" control. Should the voltage "line out", the position of the electrode is temporarily undefined and drive signal is stopped (unidirectional) or reversed (bidirectional) until swing reappears. Thermal efficiency is gained by keeping the electrode as high up in the slag as possible without breaking the meniscus.

7.0 FUTURE DEVELOPMENTS

The most important development in solidification control of wrought Alloy 718 in the next five years is expected to be in VAR. The old standard secondary melting process will get a face lift from the microprocessor revolution. All pertinent process parameters will be digitized and stored on computer disk files, enabling statistical analysis to be applied to the review of process records. Once the process capability limits are determined for each parameter, the principles of statistical process control will be applied, which will result in more consistent and uniform solidification. At first, the average parameters will become more consistent from melt to melt. As experience is gained, developers will learn how to minimize fluctuations within a melt and produce an ingot solidified uniformly from end to end, neglecting start up and hot-top effects. The success of this development will accelerate the evolution of optimum control parameter set points.

The emphasis on Statistical Process Control (SPC) will make it more difficult for the emerging processes like ESR, VADER,

EB and Plasma to overtake VAR. If enough VIM-ESR-VAR 718 is manufactured, ESR will be the next after VAR to become a statistically controlled process, which could pave the way for qualification of VIM-ESR. The combination of VIM, ESR, and VADER is intriguing, because the ESR gives a high level of cleanliness and VADER gives a high level of structural uniformity.

The video revolution should find application in the study of VAR melt zone phenomena. Other than this, no speculation is made here as to what break throughs might occur in detection of melting characteristics.

8.0 REFERENCES

1. R. G. Menzies and C. B. Adasczik, Proc. Vac. Met. Conf. on Specialty Metals Melting and Processing, Pittsburgh, PA, June 9-11, 1986, pp. 65-73, Iron and Steel Soc., 1987.
2. K. O. Yu, F. H. Soykan, and C. B. Adasczik, Proc. of 7th ICVM, November, 1982, Tokyo, Japan, pp. 1282-1289.
3. K. O. Yu., C B. Adasczik, G. J. Stelma & G. E. Maurer, Reference 1, pp. 167-174.
4. Special Metals Corporation, unpublished findings.
5. F. J. Zanner, Met. Tran., 10B, June, 1979, pp. 133-141.
6. F. J. Zanner, L. A. Bertram, and R. L. Williamson, Reference 1, pp. 49-54.
7. J. A. Domingue and K. O. Yu, Electroslag Technology, E. O. Paton Electric Welding Inst. Kiev, USSR, 1988, pp. 168-176.
8. K. O. Yu and H. D. Flanders, Proc. Vac. Met. Conf. on Specialty Metals and Melt.& Proc., Pittsburgh, PA, June 11-13, 1984, pp. 107-118, Bhat and Lherbier, Eds., Iron and Steel Soc., 1985.
9. K. O. Yu, Chinese Journal of Materials Science, Vol. 18A, No. 2, pp. 111-116 (1986).
10. M. C. Flemings and G. E. Nereo, Trans. Met. Soc. AIME, 212, 1967, p. 1449.
11. S. Kou, D. R. Poirer and M. C. Flemings, Met. Trans. B, 1978, p. 711.
12. S. Kou, D. R. Poirer and M. C. Flemings, Electric Furnace Proceedings, 1977, 35, p. 221.
13. J. A. Domingue, K. O. Yu and H. D. Flanders, NASA Conf. Publication 2337, pp. 139-149, 1984.
14. K. O. Yu, J. A. Domingue and H. D. Flanders, Proc. 8th Int. Conf. on Vac. Met., Linz, Austria, September 30-October 4, 1985, pp. 1279-1291.
15. K. O. Yu, J. A. Domingue, G. E. Maurer and H. D. Flanders, Journal of Metals, 38, (1), January, 1986, pp. 46-50.
16. H. L. Eiselstein, Advances in Tech. of Stainless Steels and Related Alloys, ASTM STP 369, 1965, pp. 62-79.
17. J. F. Wadier, G. Raisson, J. Moriet, Reference 8, pp. 119-126.
18. A. Mitchell, Reference 1, pp. 55-61.
19. D. Apelian and W. H. Sutton, Superalloys 1984, M. Gell, et. al., Eds., Amer. Soc. for Metals, 1984, pp. 421-432.
20. W. H. Sutton and S. O. Mancuso, "Electron Beam Melting & Refining - State-of-the-Art 1985," pp. 36-60, Bakish Ed., Bakish Materials Corp., Englewood, NJ, 1985.
21. W. H. Sutton, ibid, pp. 147-159.
22. W. H. Sutton and J. R. Morri, Proc. 31st Ann. Mtg. Investment Casting Inst., pp. 9:01 - 9:21, ICI, Houston, TX, 1983.
23. J. A. Domingue, F. A. Schweizer, and K. O. Yu, J. Vac. Sci. Tech. AS (4) July/August 1987, pp. 2665-2671.
24. K. O. Yu, Reference 8, pp. 83-92.
25. L. G. Hosameni, W. E. Hood, and J. H. Devletian, these proceedings.
26. F. J. Zanner, Met. Trans., 12B, December, 1981, pp. 721-728.
27. F. J. Zanner, L. A. Bertram, R. Harrison, and H. D. Flanders, Met. Trans., 17B, June, 1986, pp. 357-365.